SURFACE WAVES IN A VISCOUS LIQUID WITH CAPILLARITY

by

Peder A. Tyvand

Abstract.

The linear Lamb-Chandrasekhar theory of surface waves damped by viscosity is generalized to account for surface tension. The general dispersion relation is found by an appropriate transformation of the wave number. A dimensionless surface tension is defined by means of the gravitational acceleration and the viscosity and density of the liquid. A critical value of 2.815855 for this dimensionless surface tension is computed. Only above this value travelling ripples may exist, with group velocity exceeding phase velocity.

1. INTRODUCTION

Already Tait (1890) studies surface waves under the combined influence of capillarity and viscosity. Lamb (1932, p. 626) gave a brief treatment of this subject. Since then, the interest in waves with capillarity and viscosity appears to have subsided. This is strange in light of the fact that surface tension as well as frictional effects are most important for short waves.

However, much research has been reported on the isolated effects of surface tension and viscosity on surface waves. A series of papers on the effects of surface tension has recently been published by Hogan (1979, 1980, 1981). The basic linear theory on the influence of viscosity, given by Lamb (1932, p. 625) was elaborated further by Chandrasekhar (1955). Chandrasekhar also studied the effects of viscosity on the Rayleigh-Taylor instability (Lord Rayleigh 1883, Taylor 1950), which may be considered as the unstable counterpart to surface waves, corresponding to reversing gravity.

Bellman & Pennington (1954) investigated the combined influence of surface tension and viscosity on the Rayleigh-Taylor instability. Their results for the effects of viscosity were derived independently and more generally by Chandrasekhar (1955). In the present paper it is shown that Chandrasekhar's theory may easily be extended to account for surface tension, by a transformation of the wave number. This is true for surface waves as well as Rayleigh-Taylor instability, although different transformations apply to the two cases.

Recently, considerable attention has been given to friction-dominated gravitational flows where surface tension is important, see Cruickshank & Munson (1981) and Huppert (1982). These authors studied interesting instabilities in the creeping motion regime, where no wave propagation is possible. Also in the present problem

a convergence towards creeping motion takes place, for large wave numbers. The limit solution of creeping motion was first found by Tait (1890).

In inviscid fluids without capillarity, surface waves always have group velocity smaller than phase velocity. But with capillarity included, no matter how small, sufficiently short waves will have group velocity larger than phase velocity, see Lamb (1932, p. 460). The inclusion of viscosity introduces a lower limit on the capillarity being able to give travelling waves with group velocity exceeding phase velocity. This is because too short waves are unable to propagate, but decay locally (Chandrasekhar 1955). This critical capillarity is calculated in the present paper.

2. MATHEMATICAL FORMULATION

We consider a Newtonian liquid with a free surface in the gravity field. Cartesian coordinates are introduced with the xy-plane in the undisturbed surface and the z-axis upwards in the gravity field. g denotes the gravitational acceleration. The liquid is unbounded horizontally and its depth is taken as infinite. The dynamic viscosity, density and surface tension of the liquid are denoted by μ, ρ and T, respectively.

We consider two-dimensional motion in x and z, governed by the stream function $\phi(x,z,t)$, where t is time. As a solution of the linearized problem we first take the Fourier component

$$\phi = Z(z)e^{\sigma t}\cos kx \tag{2.1}$$

where σ is a complex time factor

$$\sigma = \sigma_r + i\sigma_i . \tag{2.2}$$

We are going to study the dispersion relation

$$\sigma_i = \sigma_i(k). \tag{2.3}$$

The real and imaginary parts of (2.1) describe two standing oscillations with decaying amplitudes. By an appropriate superposition we get the solution for one Fourier component of a wave group travelling in +x-direction;

$$\phi = Z(z)\exp(\sigma_r t)\cos k(x - \frac{\sigma_i}{k} t) \tag{2.4}$$

where its phase velocity is given by

$$c = \sigma_i/k. \tag{2.5}$$

The energy propagates with the group velocity given by

$$c_g = \frac{d\sigma_i}{dk}. \tag{2.6}$$

We have chosen a spatially periodic solution, which implies that surface waves decay in time:

$$\sigma_r < 0. \tag{2.7}$$

From the linearized Navier-Stokes equations we find the equation for $Z(z)$;

$$[(D^2-k^2)^2 - \frac{\sigma}{\nu}(D^2-k^2)]Z=0 \tag{2.8}$$

where $D \equiv d/dz$, and $\nu(=\mu/\rho)$ denotes the kinematic viscosity of the liquid. The linearized boundary conditions are:

$$(D^2+k^2)Z = 0, \quad z = 0 \tag{2.9}$$

$$[\nu\sigma(D^3-3k^2D)-\sigma^2D-gk^2 - \frac{T}{\rho}k^4]Z = 0, \quad z = 0. \tag{2.10}$$

Following Chandrasekhar (1955), a new variable y is introduced:

$$y = (1 + \frac{\sigma}{\nu k^2})^{\frac{1}{2}}. \tag{2.11}$$

It is determined by the quartic equation

$$y^4+2y^2-4y+1+ \frac{g}{k^3\nu^2} + \frac{T}{\rho k \nu^2} = 0. \tag{2.12}$$

As found by Chandrasekhar (1955) gravity and viscosity scale the kinematics of the problem, providing the length unit $\nu^{2/3}/g^{1/3}$ and the time unit $\nu^{1/3}/g^{2/3}$. Accordingly, the dimensionless wave number $\hat{k}$ and time factor $\hat{\sigma}$ are defined by:

$$(\hat{k}, \hat{\sigma}) = (\frac{\nu^{2/3}}{g^{1/3}}k, \frac{\nu^{1/3}}{g^{2/3}}\sigma) \tag{2.13}$$

The dimensionless phase and group velocities are;

$$\hat{c} = \frac{\hat{\sigma}_i}{\hat{k}} = \frac{c}{(g\nu)^{1/3}}$$

$$\hat{c}_g = \frac{d\hat{\sigma}_i}{d\hat{k}} = \frac{c_g}{(g\nu)^{1/3}} \qquad (2.14)$$

respectively. (2.11) may be rewritten as:

$$y = (1+\hat{\sigma}/\hat{k}^2)^{\frac{1}{2}}. \qquad (2.15)$$

The equation for y is now;

$$y^4+2y^2-4y+1+\hat{k}^{-3}+\hat{T}\hat{k}^{-1} = 0 \qquad (2.16)$$

where we have introduced the dimensionless surface tension:

$$\hat{T} = \frac{\rho^{1/3}}{g^{1/3}\mu^{4/3}} T = (g\nu^4)^{-1/3} \frac{T}{\rho}. \qquad (2.17)$$

$\hat{T}$ will also be termed a capillarity parameter for a viscous liquid in the gravity field. It may be considered as a fluid property when g is given.

3. TRANSFORMATION TO CHANDRASEKHAR'S PROBLEM

The equations (2.15) & (2.16) above state the mathematical problem for surface waves in dimensionless form. This problem may be reformulated in terms of the transformed wave number $\overset{*}{k}$ defined by:

$$\overset{*}{k}^{-3} = \hat{k}^{-3} + \hat{T}\hat{k}^{-1}. \tag{3.1}$$

In fig. 1 the transformed wave number $\overset{*}{k}$ is displayed as a function of the ordinary dimensionless wave number $\hat{k}$ for some values of $\hat{T}$. The equation for y is now:

$$y^4 + 2y^2 - 4y + 1 + \overset{*}{k}^{-3} = 0 \tag{3.2}$$

where y may be written:

$$y = (1 + \overset{*}{\sigma}/\overset{*}{k}^2)^{\frac{1}{2}}. \tag{3.3}$$

A transformed time factor $\overset{*}{\sigma}$ is hereby introduced, defined by

$$\overset{*}{\sigma} = \frac{\overset{*}{k}^2}{\hat{k}^2}\,\hat{\sigma}. \tag{3.4}$$

The mathematical problem for $\overset{*}{\sigma} = \overset{*}{\sigma}(\overset{*}{k})$ is now identical to the case of zero surface tension, solved by Chandrasekhar (1955). For details concerning the selection of physically relevant solutions of eq. (3.2), we refer to his paper.

Let us discuss briefly the statically unstable configuration obtained from the surface wave problem by replacing g by $-g$. Through (2.13) this corresponds to replacing $\hat{k}$ by $-\hat{k}$ and $\hat{T}$ by $-\hat{T}$. Surface tension is eliminated from the mathematical problem by the transformation

$$\overset{*}{k}^{-3} = -\hat{k}^{-3} + \hat{T}\hat{k}^{-1}. \tag{3.5}$$

This equation replaces (3.1) while eqs. (3.2)-(3.4) are retained. Static instability gives one wave number of neutral stability:

$$\hat{k}_n = \hat{T}^{-\frac{1}{2}}. \tag{3.6}$$

Only for $\hat{k} < \hat{k}_n$ the statically unstable configuration gives a Rayleigh-Taylor instability problem. Bellman & Pennington (1954) has investigated this problem for zero and nonzero surface tension. The transformation (3.5) provides a systematic background for their results. It also shows that the statically unstable configuration is stabilized due to surface tension when $\hat{k} > \hat{k}_n$, and the mathematical problem is then transformed to the surface wave problem.

The rest of this paper is devoted to surface waves. The general relation $\overset{*}{\sigma} = \overset{*}{\sigma}(\overset{*}{k})$ is given by Chandrasekhar's results, which are included in figs. 2 and 3. In fig. 2 the absolute value of the decay rate $\overset{*}{\sigma}_r(\overset{*}{k})$ is shown, and in fig. 3 the dispersion relation $\overset{*}{\sigma}_i(\overset{*}{k})$. In the latter figure the phase and group velocities for the case $\hat{T} = 0$ are included, based on new calculations (see chapter 4). Here the group velocity is always smaller than the phase velocity, but this is no longer true when $\hat{T}$ exceeds a critical value.

The solid curves in fig. 2 represent the surface wave problem. The decay rate has two branches for $\overset{*}{k} > \overset{*}{k}_b$ where the branch point is given by

$$\overset{*}{k}_b = 1.1981 \tag{3.7}$$

found by Chandrasekhar (1955). For $\overset{*}{k} < \overset{*}{k}_b$ we have two complex conjugate solutions for $\overset{*}{\sigma}$, corresponding to waves propagating in + and -x-direction. For $\overset{*}{k} > \overset{*}{k}_b$ we have only local decay of surface disturbances; no travelling waves exist and $\overset{*}{\sigma}$ is real. The upper branch for $\overset{*}{\sigma}_r$ represents the rapidly decaying "viscous" mode.

The lower branch represents the "creeping" mode, which converges towards the creeping motion solution as $\overset{*}{k}$ increases. The creeping motion solution, where inertial terms in the equation of motion are neglected, is also included in fig. 2 as the dotted curve. This is a common asymptotic limit for our wave problem and the Rayleigh-Taylor instability, the latter being represented by the dashed curve in fig. 2. The decay/growth rate for creeping motion is

$$|\overset{*}{\sigma}_r| = \frac{1}{2\overset{*}{k}} \tag{3.8}$$

and was first calculated by Tait (1890). In this equation, as for all curves in fig. 2, the dependence on surface tension is hidden in the transformation equations (3.1) and (3.5).

Expressed in the transformed quantities, the convergence towards the creeping motion solution is independent of surface tension. The deviations from the creeping motion solution (3.8) are below 5% for $\overset{*}{k} > 2.0$ and below 1.5% for $\overset{*}{k} > 3.0$. $|\overset{*}{\sigma}_r|$ for Rayleigh-Taylor instability is always smaller than for creeping motion, because the released potential energy is needed not only to overcome viscosity, but also to accelerate the fluid. For surface waves $|\overset{*}{\sigma}_r|$ is always larger than for creeping motion.

4. CALCULATION OF THE CRITICAL CAPILLARITY PARAMETER

The critical value of the capillarity parameter is denoted by $\hat{T}_c$. When $\hat{T} < \hat{T}_c$ we always have $\hat{c}_g < \hat{c}$. When $\hat{T} > \hat{T}_c$ there is a finite interval of wave numbers for which $\hat{c}_g > \hat{c}$. At $\hat{T} = \hat{T}_c$ there is just one wave number $\hat{k}_c$ for which $\hat{c}_g = \hat{c}$, while all other wave numbers give group velocity smaller than the phase velocity.

The results given by Chandrasekhar (1955) are not sufficiently detailed for computing $\hat{T}_c$. Therefore eq. (2.16) has been solved numerically for various values of $\hat{k}$ and $\hat{T}$. An IMSL-routine of a CYBER 170 computer has been applied.

The group velocity has been approximated by

$$\hat{c}_g \approx \frac{\Delta\hat{\sigma}}{\Delta\hat{k}} \tag{4.1}$$

where the deltas denote forward differences. The choice $\Delta\hat{k} = 10^{-4}$ is sufficiently small for the drawing accuracy in figs. 3-5. However, for computing $\hat{T}_c$, the approximation (4.1) gives the dominating numerical error unless $\Delta\hat{k}$ is of order 10^{-6} or less. Successive approximations for $\hat{T}_c$ and $\hat{k}_c$ based on comparisons between the results for $\hat{c}$ and $\hat{c}_g$ (with $\Delta\hat{k} = 10^{-6}$) have given the results:

$$\begin{aligned} \hat{T}_c &= 2.8158553 \pm 0.0000002 \\ \hat{k}_c &= 1.5805 \pm 0.0001. \end{aligned} \tag{4.2}$$

An improved calculation is though possible, based on the fact that $\hat{c}_g = \hat{c}$ is equivalent to

$$\frac{d\hat{c}}{d\hat{k}} = 0. \tag{4.3}$$

When $\hat{T} < \hat{T}_c$ the phase velocity is a monotonous function of $\hat{k}$, while there are two extremal points when $\hat{T} > \hat{T}_c$. At $\hat{T} = \hat{T}_c$ there is just one stationary point (inflexion point) for $\hat{c}$, at the wave number $\hat{k} = \hat{k}_c$. The method is here just to compare successive values of $\hat{c}$ for small increments in $\hat{k}$, and select the case with one stationary point. The most refined calculations are given in table 1. The step length chosen here for the wave number is so small that numerical errors are revealed. Interpolations based on table 1 give the final critical values

$$\hat{T}_c = 2.81585531 \pm 0.00000002$$
$$\hat{k}_c = 1.58047 \pm 0.00003 \qquad (4.4)$$

The time factor for this critical mode is given by

$$(\hat{\sigma}_r, \hat{\sigma}_i) = (-1.7385,\ 2.0417) \qquad (4.5)$$

with the common value of phase and group velocities

$$\hat{c} = \hat{c}_g = 1.2918. \qquad (4.6)$$

Fig. 4 shows the dispersion relation with the phase and group velocities as functions of $\hat{k}$ for $\hat{T} = 3.42$, a value above the critical capillarity. The group velocity slightly exceeds the phase velocity in the interval $1.09 < \hat{k} < 2.47$. For the dispersion relation $\hat{\sigma}_i(\hat{k})$ the stretching and distorting effects of the transformations (3.1) & (3.3) are observed on comparing fig. 4 with fig. 3.

Fig. 5 gives a division of the $\hat{T},\hat{k}$ plane into three different regions. The unshaded area above the branch point $\hat{k}_b$ does not allow any travelling waves. Below the solid curve for the branch point we have travelling waves; In the shaded area these waves have group velocity smaller than their phase velocity. The dotted area

shows the "ripple" region where the group velocity exceeds the phase velocity. The boundary of this ripple region is represented by the dashed curve defined by $\hat{c}_g = \hat{c}$ (or equivalently $\frac{d\hat{c}}{d\hat{k}} = 0$). For $\hat{T} >> 1$ the upper and lower branches of the dashed curve are approximately given by the equations

$$\hat{k} = 0.79\ \hat{T}, \quad \hat{k} = 3.8\ \hat{T}^{-1} \tag{4.7}$$

respectively. The branch point $\hat{k}_b$ is also a linear function when $\hat{T} >> 1$. Its angle coefficient is 1.72, about twice that of the upper boundary curve for the ripple region.

The solid curves in fig. 6 show the common values of $\hat{c}$ and $\hat{c}_g$, which define the boundaries of the ripple region. These values are also the local maximum and minimum for $\hat{c}$. The local maximum for $\hat{c}_g$ is given by the dashed curve, and the dotted curve represents the corresponding phase velocity. The dotted curve is relatively close to the curve for maximum phase velocity, and the difference between the group and phase velocities shown in fig. 6 is not maximal.

5. CONCLUSIONS

The present theory has been derived for spatially periodic waves decaying in time. But within linear theory the results may be carried over to steady waves generated by a moving disturbance. Such waves have spatial instead of temporal decay. When $\hat{T} < \hat{T}_c$ a moving two-dimensional disturbance is unable to carry travelling ripples in front of itself. Because the group velocity is always smaller than the phase velocity, all wave energy must propagate downstream. When $\hat{T} > \hat{T}_c$ a wave group capable of propagating upstream may exist. The width of its spectrum increases with $\hat{T}$ (see fig. 5).

In the viscous fluid jet buckling experiments by Cruickshank & Munson (1981), the available values of $\hat{T}$ range between 0.00245 and 0.0502. These values are far below our critical value 2.815855. This indicates that viscous jet buckling occurs only for fluids where travelling ripples cannot exist.

REFERENCES

Bellman, R. & Pennington, R. H., 1954. Effects of surface tension and viscosity on Taylor instability.
Quart. J. Appl. Math. 12, 151-162.

Chandrasekhar, S., 1955. The character of the equilibrium of an incompressible heavy viscous fluid of variable density.
Proc. Camb. Phil. Soc. 51, 162-178.

Cruickshank, J. O. & Munson, B. R., 1981. Viscous fluid buckling of plane and axisymmetric jets.
J. Fluid Mech. 113, 221-239.

Hogan, S. J., 1979. Some effects of surface tension on steep water waves.
J. Fluid Mech. 91, 167-180.

Hogan, S. J., 1980. Some effects of surface tension on steep water waves. Part 2.
J. Fluid Mech. 96, 417-445.

Hogan, S. J., 1981. Some effects of surface tension on steep water waves. Part 3.
J. Fluid Mech. 110, 381-410.

Huppert, H. E., 1982. Flow and instability of a viscous current down a slope.
Nature 300, 427-429.

Lamb, H., 1932. Hydrodynamics.
Cambridge University Press.

Rayleigh, Lord, 1883.
Proc. Lond. Math. Soc. 14, 170-177; also, Scientific Papers, vol. 2, pp. 200-207.

Tait, P. G., 1890. Note on ripples in a viscous liquid.
Proc. Roy. Soc. Edin. 17, 110-115.

Taylor, G. I., 1950. The instability of liquid surfaces when accelerated in a direction perpendicular to their planes.
I. Proc. Roy. Soc. A 201, 192-196.

N	$\hat{k}_N$	$[\hat{c}(\hat{k}_N)-\hat{c}(\hat{k}_{N-1})]\times 10^{16}$		
		for $\hat{T}$=2.8158552	for $\hat{T}$=2.8158553	for $\hat{T}$=2.8158554
1	1.58020			
2	1.58023	-7532	-4192	-213
3	1.58026	-7105	-3268	213
4	1.58029	-6182	-2629	995
5	1.58032	-5755	-2061	1421
6	1.58035	-5258	-1421	2274
7	1.58038	-4761	-1137	2558
8	1.58041	-4619	-924	2629
9	1.58044	-4263	-995	2984
10	1.58047	-4405	-213	3126
11	1.58050	-4121	-639	3055
12	1.58053	-4405	-924	2842
13	1.58056	-4476	-782	2771
14	1.58059	-5116	-1066	2416
15	1.58062	-5045	-1776	2061
16	1.58065	-5826	-2203	1421
17	1.58068	-6466	-2629	995
18	1.58071	-6963	-3411	284
19	1.58074	-7674	-4263	-568
20	1.58077	-8669	-5045	-1563

Table 1. Sample points N for the dimensionless wave number $\hat{k}$ and corresponding increments in the dimensionless phase velocity $\hat{c}$ for some values of $\hat{T}$ in the vicinity of its critical value $\hat{T}_c$.

Figure legends.

Fig. 1 Transformed wave number $\overset{*}{\hat{k}}$ as a function of the dimensionless wave number $\hat{k}$ for the surface wave problem. Values of the dimensionless surface tension $\hat{T}$ equal to 0, 0.1, 1 and 10 are represented.

Fig. 2 Absolute values of the transformed grouth/decay rate, $|\overset{*}{\sigma}_r|$, as functions of the transformed wave number $\overset{*}{\hat{k}}$. Solid curves show surface waves. Dashed curve shows Rayleigh-Taylor instability. Dotted curve shows creeping motion solution.

Fig. 3 Solid curve shows dispersion relation $\overset{*}{\sigma}_i(\overset{*}{\hat{k}})$ for the transformed surface wave problem. The other curves are reserved for the case $\hat{T} = 0$. Dashed curve shows phase velocity $\hat{c}(\hat{k})$. Dashed and dotted curve shows group velocity $\hat{c}_g(\hat{k})$.

Fig. 4 Surface wave problem for $\hat{T} = 40^{1/3} = 3.42$. Solid curve shows dispersion relation $\hat{\sigma}_i(\hat{k})$. Dashed curve shows phase velocity $\hat{c}(\hat{k})$. Dashed and dotted curve shows group velocity $\hat{c}_g(\hat{k})$.

Fig. 5 Regions of different solutions in the $\hat{T},\hat{k}$ plane for the surface wave problem. Unshaded area: No travelling waves, local decay only. Solid curve: Branch point $\hat{k}_b(\hat{T})$. Shaded area: Travelling waves have group velocity smaller than phase velocity. Dashed curve: $\hat{c}_g = \hat{c}$. Dotted area: Travelling waves with group velocity greater than phase velocity.

Fig. 6 Dimensionless phase velocity $\hat{c}$ and group velocity $\hat{c}_g$ as functions of $\hat{T}$. Solid curves are given by $\hat{c} = \hat{c}_g$. Dashed curve shows the local maximum of $\hat{c}_g$ in the ripple region, and dotted curve shows the corresponding value of $\hat{c}$.

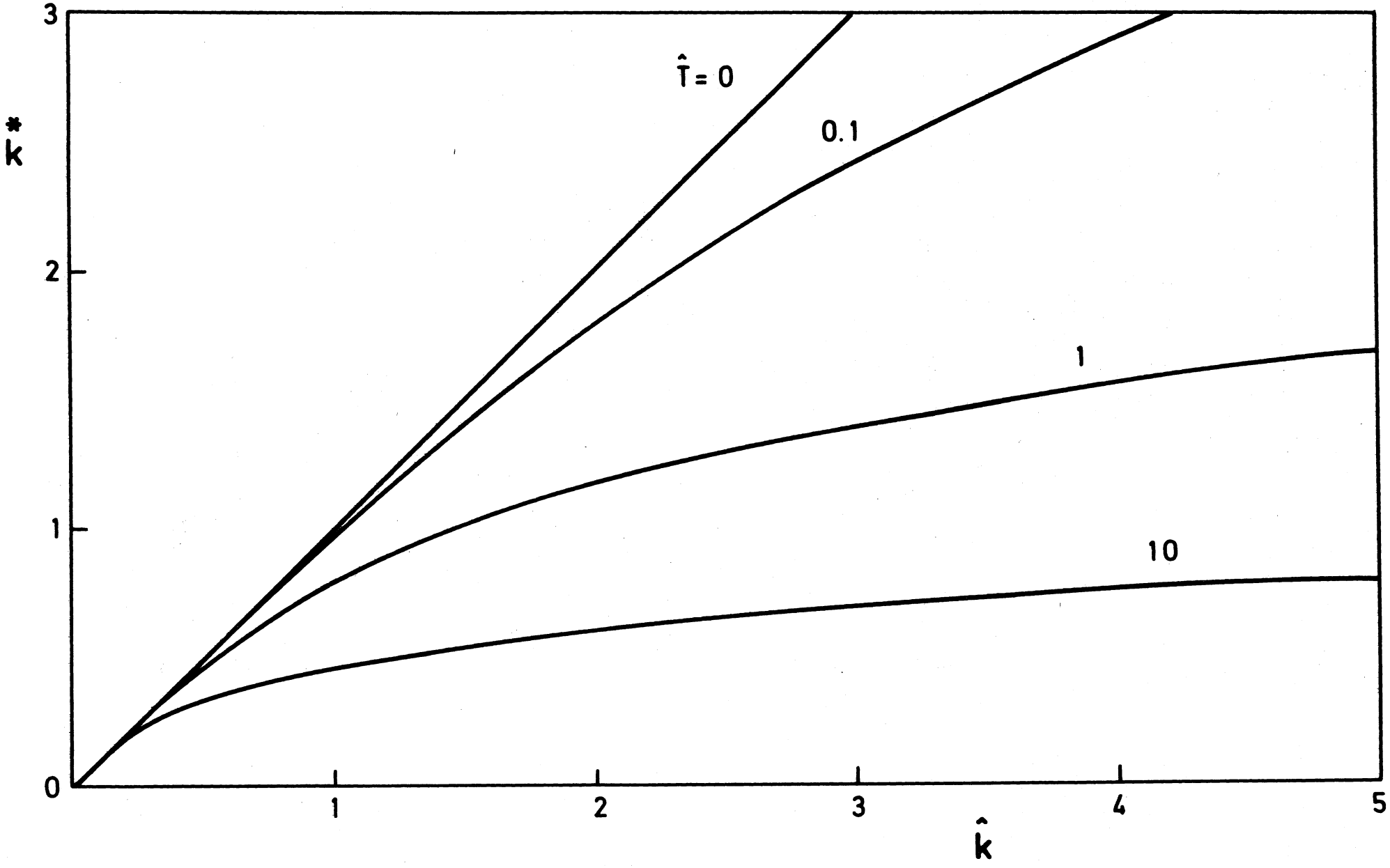

FIG. 1

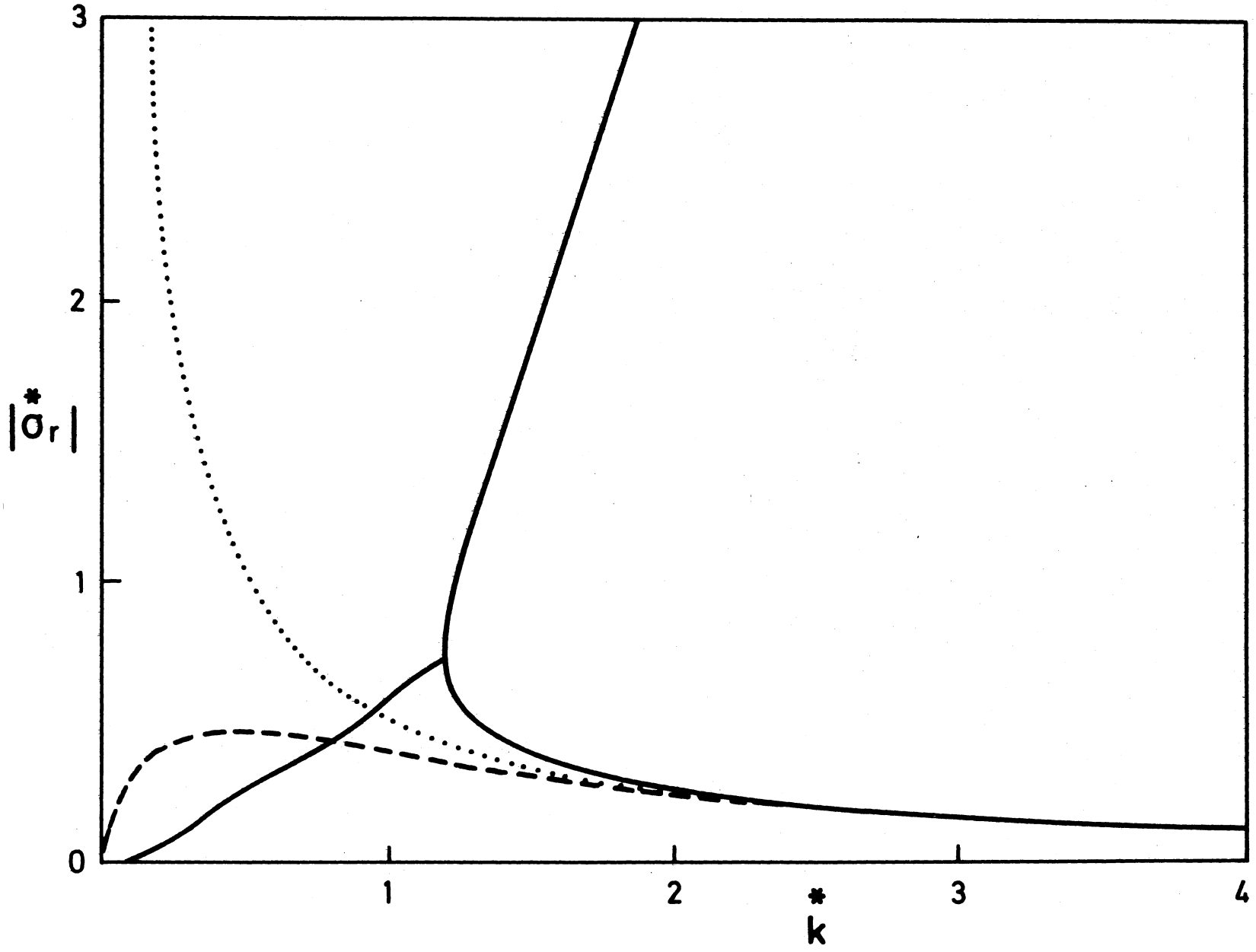

FIG. 2

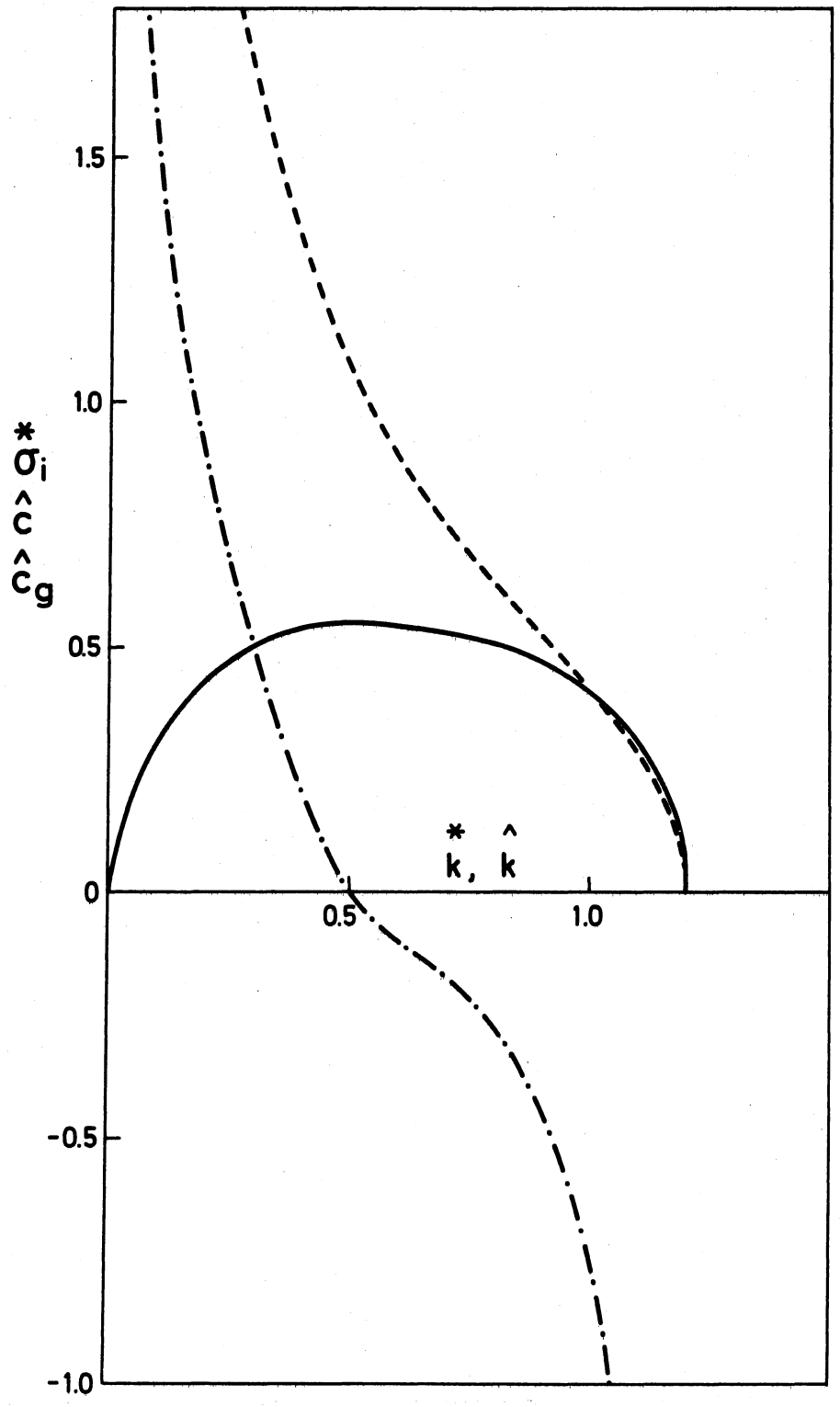

FIG. 3

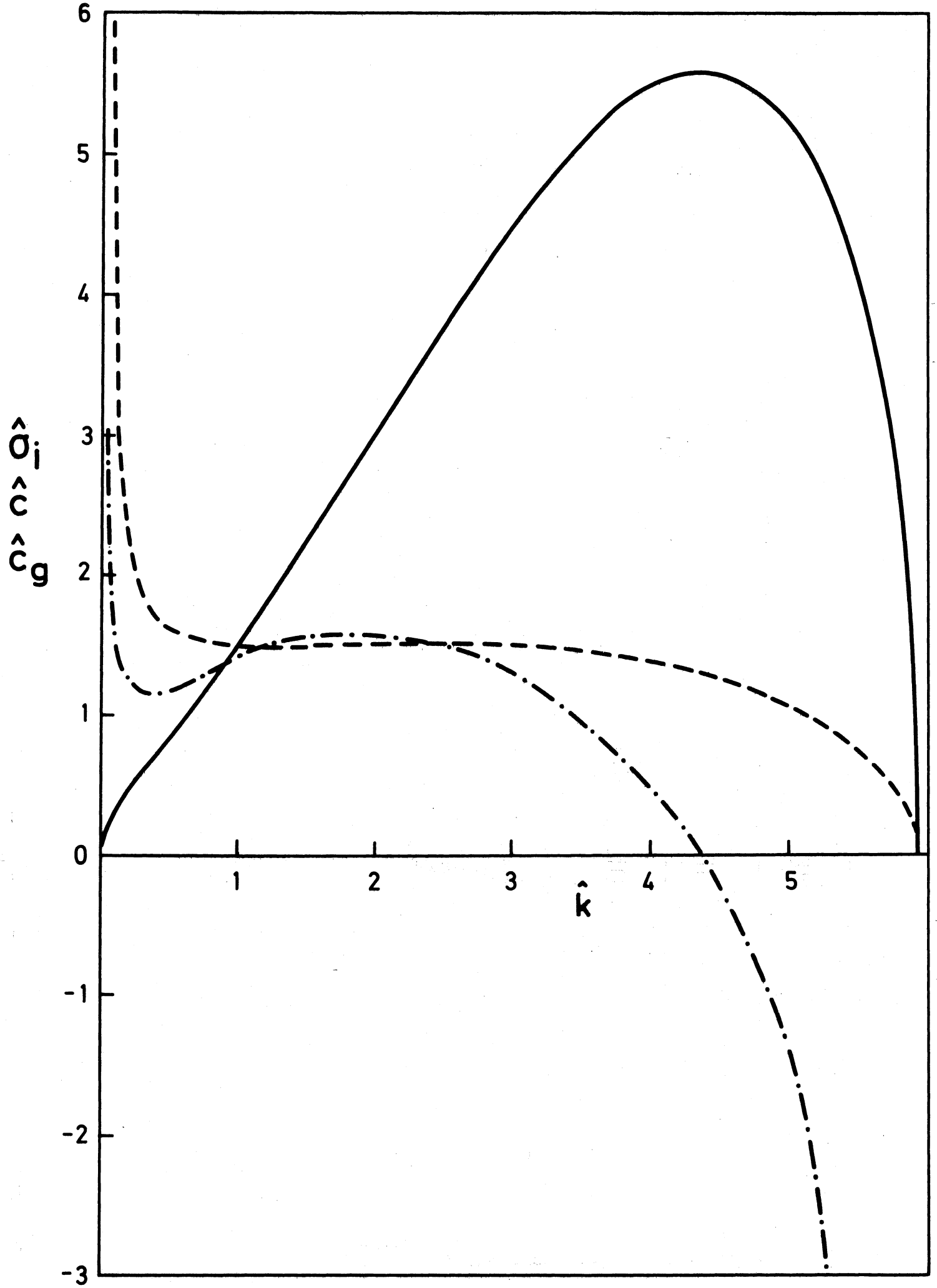

FIG. 4

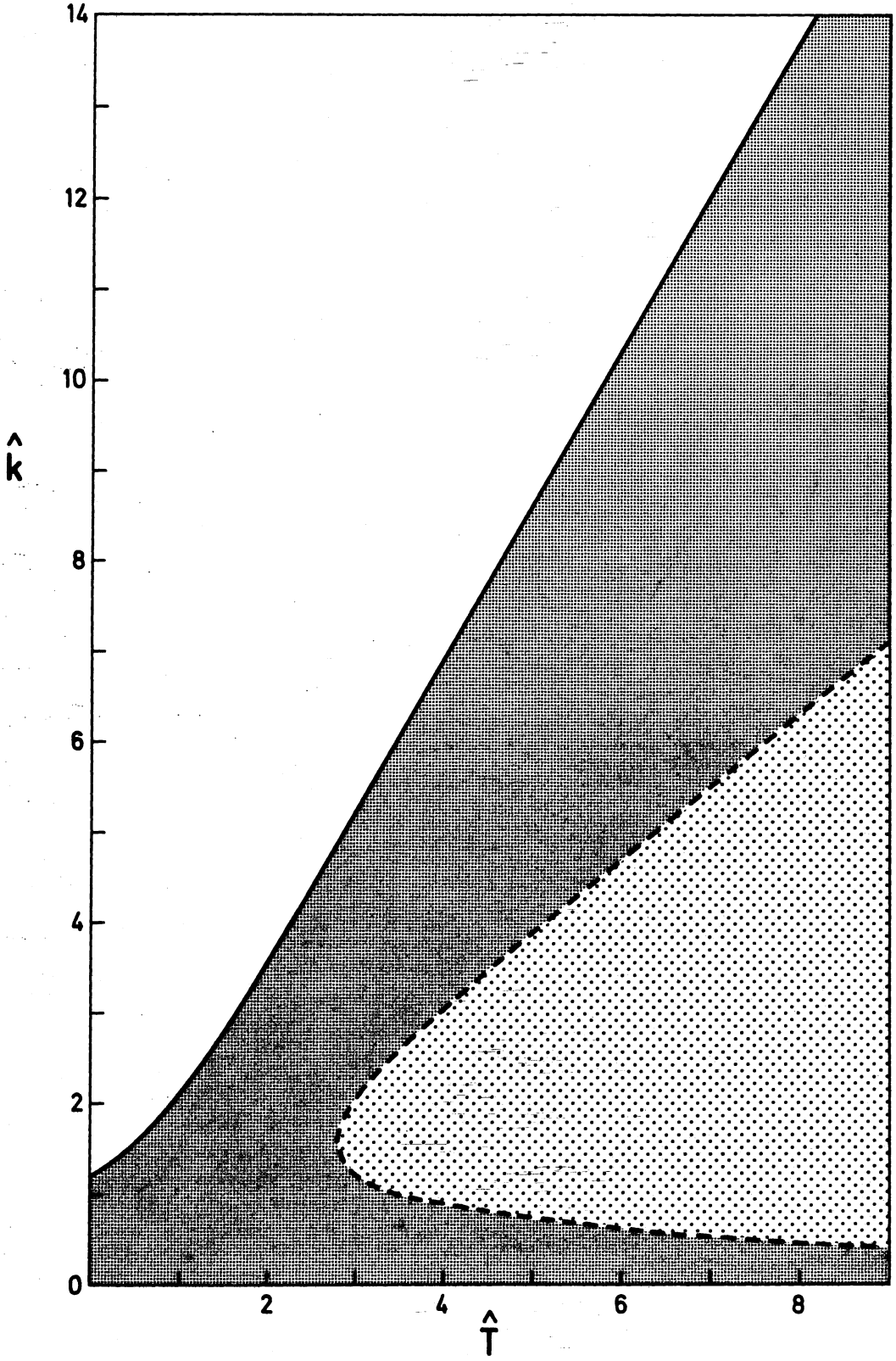

FIG. 5

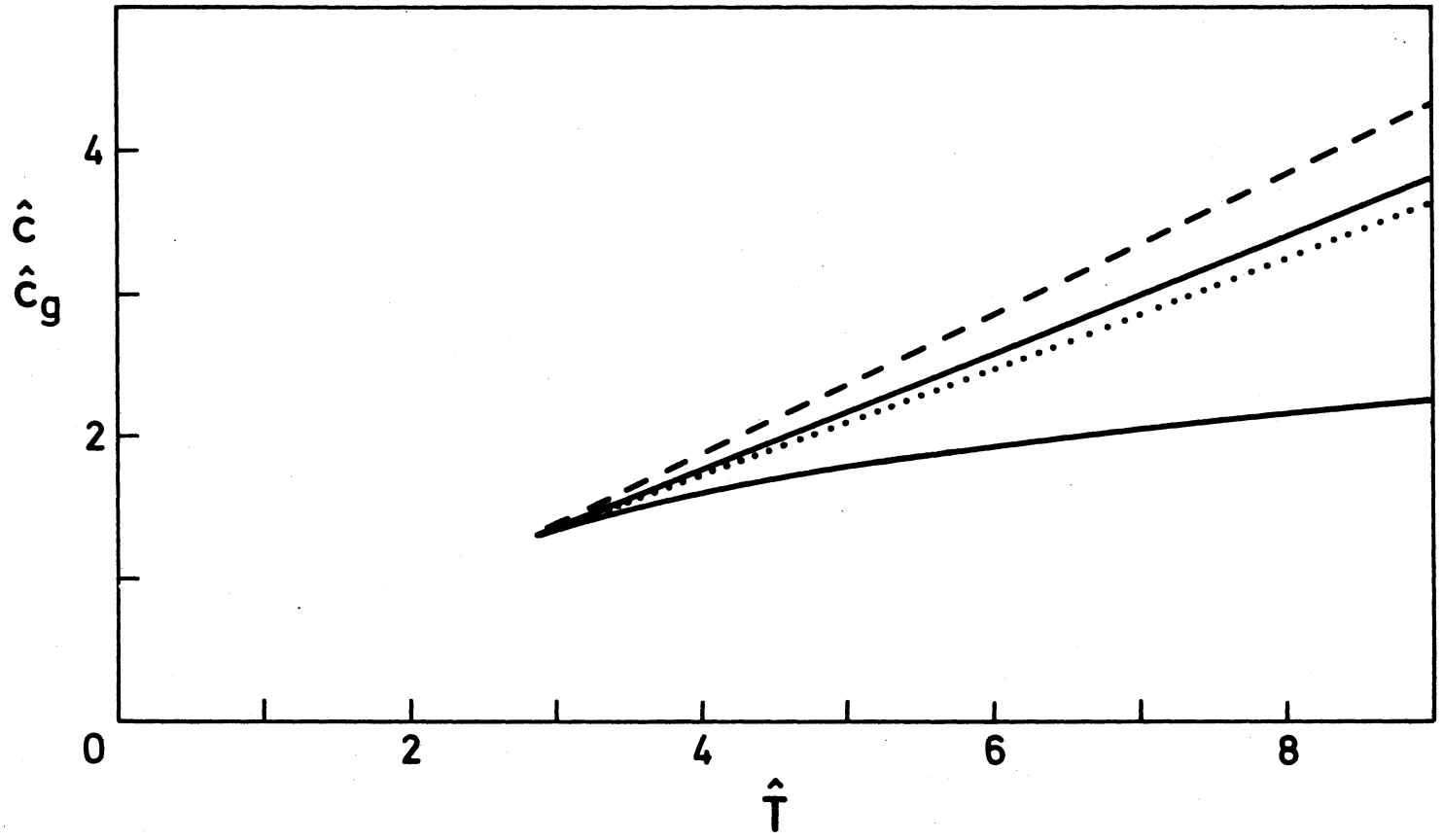

FIG. 6